

# Removal of Spurious Admixture in a Self-consistent Theory of Adiabatic Large Amplitude Collective Motion

Toby D. Young\* and Niels R. Walet†

*School of Physics and Astronomy, The University  
of Manchester, Manchester, M60 1QD, U.K.*

(Dated: July 15, 2018)

## Abstract

In this article we analyse, for a simple model, the properties of a practical implementation of a fully self-consistent theory of adiabatic large-amplitude collective motion using the local harmonic approach. We show how we can deal with contaminations arising from spurious modes, caused by standard simplifying approximations. This is done both at zero and finite angular momentum. We analyse in detail the nature of the collective coordinate in regions where they cross spurious modes and mixing is largest.

PACS numbers: 21.60.-n, 21.60.Ev, 21.60.Jz

---

\*Electronic address: [young@theory.phy.umist.ac.uk](mailto:young@theory.phy.umist.ac.uk)

†Electronic address: [niels.walet@manchester.ac.uk](mailto:niels.walet@manchester.ac.uk)

## I. INTRODUCTION

One of the long-standing concerns in nuclear structure theory is to understand how the collective properties of a microscopic many-body system emerge from the behaviour of its many quantal constituents [1, 2]. Bohr's liquid drop model can be used to describe many collective modes [3] and still provides us with the concepts used in most discussions of collective motion. Clearly, a more microscopic method to describe such modes has been sought and many methods exist that try to describe collective motion.

One method commonly used is based on a mean-field approach, the Constrained Hartree-Fock-Bogoliubov (CHFB) method [2]. Here a collective energy surface is generated by mapping the energy expectation value as a function of the expectation values of a small number of one-body operators (mean-field constraints). The principal weakness of CHFB is that the collective motion of the nucleus is determined without any dynamical criterion for choosing one particular constraint (collective operator) over another. Often the choice is inspired by the Bohr Hamiltonian, and one uses only quadrupole and pairing operators. In nuclear physics the first applications of the CHFB were to the dominant surface vibrations [4, 5, 6, 7, 8] which called attention to the need for a more meaningful theory.

Ideally the method chosen to tackle this problem should allow the dynamics of the system to evolve through the microscopic Hamiltonian without the intervention of *ad hoc* elements forcing the system into a specific mode of oscillation. One possibility, followed in this article and discussed in detail in the review article [9], is a method that determines collective motion by following the normal modes of oscillation. This incorporates methods such as the Quasiparticle Random Phase Approximation (QRPA) [2]. Thus the low-lying physical excitations of the system using the small-amplitude harmonic limit (i.e., QRPA) are used to self-consistently determine the constraining operator. Restricting to the case of a single collective excitation, we then describe a collective path through the energy surface generated by the Hamiltonian.

Initially [9] most applications ignored pairing, and they used versions of the Hartree-Fock (HF) method. In recent years, three different models including pairing, and thus requiring the Hartree-Fock-Bogoliubov (HFB) mean-field approximation, have been investigated. The first [10, 11] describes a two crossing levels, with an additional pairing interaction. One problem first encountered in that work was that of dealing correctly with spurious

modes arising from spontaneously broken symmetries within the mean-field approximation even though for this model one can solve this problem exactly, unlike the problems discussed below. The second [12, 13] is a microscopic  $O(4)$  model with pairing and quadrupole interactions which focuses on shape coexistence phenomena in a schematic way. The third set of applications [14, 15] uses the Pairing Plus Quadrupole (PPQ) model for semi-realistic nuclei using techniques developed earlier [16]. These calculations typically use model spaces consisting of two major shells for both neutrons and protons, leading to large dimensions for the QRPA, and extremely time-consuming calculations. A balance is found by introducing a basis of operators which gives a truncated expression of the QRPA in such a way that it gives a reasonably accurate approximation of the low-lying excitations [17, 18]. This method has recently been extended to finite rotational frequencies [15].

In this paper we do not make such a truncation, but we will investigate the nature of the approximations made before doing the projection on a small basis of operators. To this end we employ a single  $j$ -shell PPQ model. The main difficulty encountered here is associated with admixtures of spurious modes (Nambu-Goldstone modes) arising in the formalism as vacuum-degenerate solutions in the excitation spectra which do not correspond to physical excitations. Though at extrema on the energy surface spurious modes do not mix with other modes, this is not necessarily true at other points on the energy surface, especially after additional approximations have been made. Since spurious modes do not correspond to physical excitations, any mixing of these modes with other excitations — we will refer to this phenomenon as ‘spurious admixture’ — can potentially lead the system away from the collective path. In order to ensure that spurious modes behave correctly far from stable equilibrium we need to modify our algorithm slightly, and the study of these modifications is the main focus of this article.

This article is organised as follows: First, in section II we give a brief overview of the Local Harmonic Approximation (LHA) followed in this article. We also give a description of our projection technique to remove spurious admixture from the formalism. Secondly, in section III, following the lead given by references [10, 11, 12, 13, 14, 15, 16, 17, 18, 19, 20, 21], the single  $j$ -shell PPQ model is presented and solved. We present our main results from testing our methods of removal of spurious admixture, as well as discussing a complementary investigation of the effect of the pairing strength on the collective potential. In the next section, Sec. IV we then study the behaviour of our techniques at finite angular momentum.

Finally, a summary and outlook is given in section V.

## II. LOCAL HARMONIC APPROXIMATION

In this section we give a brief overview of the LHA as used in this article; for a more detailed exposition of the theory see Ref. [9]. We also give a description of two methods to remove spurious admixtures from the formalism.

The LHA starts from assuming a non-relativistic many-body Hamiltonian  $H_{\text{nuclear}}$  that is capable of describing the low-energy properties of nuclear structure. By means of the time-dependent mean field approximation, the quantum problem is turned into a classical Hamiltonian problem and the description of collective motion can now be formulated fully as a classical decoupling problem. We now try to find collective coordinates such that the mixing between collective and non-collective degrees of freedom is small. The Hamiltonian contains  $N$  — the number of quasi-particle states squared — canonical pairs of coordinates  $\xi^\alpha \in \xi = \{\xi^1, \dots, \xi^N\}$  and momenta  $\pi_\alpha \in \pi = \{\pi_1, \dots, \pi_N\}$  in the Hamiltonian  $\mathcal{H} \equiv \mathcal{H}(\xi, \pi)$ . In the adiabatic limit, valid when the collective motion is slow, we Taylor expand the Hamiltonian up to second order in momenta. We find

$$\mathcal{H}(\xi, \pi) = V(\xi) + \frac{1}{2}\pi_\alpha B^{\alpha\beta}(\xi)\pi_\beta \quad . \quad (1)$$

The dynamics of the system are thus characterised by the point function  $V(\xi)$  and by the reciprocal mass tensor  $B^{\alpha\beta}$ , which also plays the role of a metric tensor.

We now change representation from the initial set of coordinates and momenta  $(\xi, \pi)$  to a new set  $(q, p)$  through point transformation, *i.e.*,  $q = f(\xi)$ , in the hope that we can approximately decouple the collective from non-collective motion. Using the standard Einstein convention — where a comma denotes a partial derivative  $f_{,\alpha} \equiv \frac{\partial f}{\partial \xi^\alpha}$  — the point transformation has the form

$$\xi^\alpha = g^\alpha(q^1, \dots, q^N) \equiv g^\alpha(q) \quad , \quad \pi_\alpha = f_{,\alpha}^\mu p_\mu \quad , \quad (2)$$

where  $g$  is the inverse of  $f$ . The Hamiltonian takes the new form

$$\mathcal{H}(\xi, \pi) = \bar{\mathcal{H}}(q, p) = \bar{V}(q) + \frac{1}{2}p_\mu \bar{B}^{\mu\nu}(q)p_\nu \quad . \quad (3)$$

Here a bar denotes the transformed potential ( $\bar{V} = V(\xi(q))$ ) and the transformed mass tensor ( $\bar{B}$ ).

The basic equation of the problem can now be derived by looking at the dynamical fluctuations at an arbitrary point in coordinate space, (the Local Harmonic Equation (LHE))

$$M_{\beta}^{\alpha} f_{,\alpha}^{\mu} = \Omega_{\mu}^2 f_{,\beta}^{\mu} \quad , \quad (4)$$

$$M_{\beta}^{\gamma} = \bar{V}_{;\alpha\beta} B^{\beta\gamma} \quad , \quad (5)$$

where a semi-colon denotes a covariant derivative. The second equation states that the force should be in the direction of one of the eigenvectors,

$$V_{,\alpha} = \lambda f_{,\alpha}^1. \quad (6)$$

For exact decoupling this direction is (co-)tangential to the collective path, but we construct an algorithm for finding cases for approximate decoupling by not imposing this as a condition. Instead, as discussed in Ref. [9], we do have a measure for the quality of collective path based on the deviations from this criterion.

In the equations above, the covariant derivative is defined using the metric  $B^{\alpha\beta}$  provided by the kinetic energy. The calculation of the covariant derivative requires the inversion of the mass matrix, which is fraught with numerical difficulties when  $B$  has zero eigenvalues. Therefore we shall make the usual assumption that we can ignore the effects of these curvature terms, i.e,  $\bar{V}_{;\alpha\beta} \sim \bar{V}_{,\alpha\beta}$ .

### A. Method of removing spurious admixture

It can be shown that for the HFB theory considered here, the LHE is a simple generalisation of the QRPA to non-equilibrium states. Thus, as in the usual equilibrium HFB plus QRPA framework spurious modes arise as artifacts of mean-field symmetry breaking. In a numerically exact calculation, without approximations, such modes decouple from the problem, and we do not have to consider them in detail. When approximations are made, especially the simplification arising when neglecting the covariant terms in the derivatives, the situation is different and we get spurious admixtures. Since these admixtures do not correspond to physical excitations we must remove their components completely from the formalism without altering the meaning of the collective coordinate. In all cases we know the spurious operator; it may correspond to a coordinate or momentum, but we do not normally know the conjugate variable.

Our method is easily generalised to include any number of spurious coordinates and is therefore not specific to the model we solve in this article. As we will see, the main difficulty with this approach is that we do not know the conjugate variables and we will therefore have to devise a way to approximate an operator for the momenta in order to complete our projection method (this is discussed below).

The first step is thus the construction of a set of approximate conjugate variables. This is best illustrated for the particle number, although other operators are dealt with similarly.

Thus we have  $q_{,\alpha} = \mathcal{N}_{,\alpha}$ , and its conjugate momentum  $p^\alpha = \phi^\alpha$ . We are looking for operators that satisfy the conditions

$$B^{\alpha\beta}\mathcal{N}_{,\beta} = 0 \quad , \quad \phi^\alpha V_{,\alpha\beta} \propto \mathcal{N}_{,\alpha} \quad . \quad (7)$$

Let us now turn to the canonical coordinates and momenta and the question of how to define the momentum variable  $\phi$  conjugate to the particle number  $\mathcal{N}$ . Naive inversion of the second equation in (7) gives

$$\phi^\beta \propto \mathcal{N}_{,\alpha} (V_{,\alpha\beta})^{-1} \quad . \quad (8)$$

We thus approximate  $\phi$  by

$$\phi^\alpha = \sum_j \frac{1}{\epsilon_j} e_j^\alpha \mathcal{N}_{,\alpha} e_\alpha^j \quad , \quad (9)$$

where  $e_\alpha^j$  are components of the eigenvectors and  $\epsilon_j$  the eigenvalues of the potential matrix. Unfortunately  $V_{,\alpha\beta}$  is usually singular due to zero eigenmodes of the QRPA matrix, and we need to replace (8) by a singular value decomposition. To this end we remove those terms in the sum corresponding to eigenvalues that are close to zero  $\epsilon_j \sim 0$ . In practise, the size of the excluded zone is found through trial and error.

Finally, we need to ensure that the operators arising from our construction are all conjugate to each other: In a generalised representation we have a set of canonical conjugate coordinates and momenta connected with spurious modes

$$q_{,\alpha}^i \quad , \quad \forall i \in \{1, 2, \dots, N_S\} \quad , \quad (10a)$$

$$p_j^\alpha \quad , \quad \forall j \in \{1, 2, \dots, N_S\} \quad , \quad (10b)$$

where  $N_S$  denotes the total number of spurious modes. For well defined coordinates and momenta we have  $q_{,\alpha}^i p_j^\alpha = \delta_j^i$ , but our construction above usually does not satisfy this (partially due to neglect of covariant terms, and partially due to numerical problems).

We start by defining the overlap matrix

$$O_j^i = q_{,\alpha}^i p_j^\alpha \quad , \quad (11)$$

which, had we have done the computation consistently, would be the identity matrix corresponding to the Poisson brackets between canonical coordinates and momenta. To achieve canonicity we now diagonalise the overlap matrix

$$(S^{-1})_l^k O_j^i S_l^j = \delta_l^k \tau_l \quad , \quad (12)$$

where  $S$  are a set of orthonormal eigenvectors and  $\tau_l$  are the eigenvalues of the system. This allows us to define a new ‘tilde’ basis

$$\tilde{q}_{,\alpha}^i = (S^{-1})_j^i q_{,\alpha}^j \quad , \quad (13)$$

$$\tilde{p}_i^\alpha = \frac{1}{\tau_j} S_j^i p_i^\alpha \quad , \quad (14)$$

satisfying the orthonormal condition  $\tilde{q}_{,\alpha}^i \tilde{p}_j^\alpha = \delta_j^i$ , used in the definition of the projection operator

$$P_\alpha^\beta = \delta_\alpha^\beta - \tilde{q}_{,\alpha}^i \tilde{p}_j^\beta \quad , \quad (15)$$

The projection matrix is now applied to the potential and mass matrices,

$$\tilde{V}_{,\alpha\beta} = P_\alpha^{\alpha'} V_{,\alpha'\beta'} P_\beta^{\beta'} \quad , \quad \tilde{B}^{\alpha\beta} = P_\alpha^\alpha B^{\alpha'\beta'} P_{\beta'}^\beta \quad . \quad (16)$$

The related QRPA eigenvalue problem has now a number of zero eigenvalues, and the spurious modes do not mix with with any other ones.

### III. MODEL AND RESULTS

In this section we solve the single  $j$ -shell PPQ model for Adiabatic Large Amplitude Collective Motion (ALACM) using the methods discussed above to remove spurious admixture. The PPQ model we use here is a good starting point despite its limitations as it is relatively simple compared to models with more realistic forces and allows us to choose a conveniently small basis set with which to work. Furthermore, we would like to ‘bridge the gap’ between simpler applications starting from a partial Hamiltonian and semi-realistic descriptions of real atomic nuclei (see discussion above).

Following reference [22] the PPQ Hamiltonian will be treated in the Hartree-Bogoliubov (HB) framework. We start with the traditional single  $j$ -shell PPQ Hamiltonian

$$\hat{H} = -\frac{1}{2}\kappa \sum_M (-1)^M : \hat{Q}_M \hat{Q}_{-M} : -\chi \hat{P}^\dagger \hat{P} \quad , \quad (17)$$

which is a straightforward two-body interaction Hamiltonian. Here colons denote normal ordering and  $\kappa$  and  $\chi$  are the coupling strength of the quadrupole and pairing interactions, respectively. We can only impose correct particle number on average, which is done by a Lagrange multiplier. When looking at non-zero angular momentum we impose an additional constraint for the expectation value of  $J_x$ .

The quadrupole and pairing operators are to be written in the simplest form possible in the original particle basis

$$\hat{Q}_M \propto \sum_{mm'} (-1)^{j-m-M} \begin{bmatrix} j & j & 2 \\ m & -m' & M \end{bmatrix} c_m^\dagger c_{m'} \quad , \quad (18)$$

$$\hat{P} = \sum_{m>0} (-1)^{j-m} c_{-m} c_m \quad , \quad (19)$$

where  $c_m^\dagger$  and  $c_m$  are creation and destruction operators on the single-particle state  $|m\rangle$ , and the object in square brackets denotes a Clebsch-Gordan coefficient. Since we are working in a single shell, we can absorb the reduced matrix element of the quadrupole operator into  $\kappa$ , and use an equality in Eq. (18) We use the definitions

$$q_M = \langle \hat{Q}_M \rangle \quad , \quad q_{\pm 1} = 0, \quad p_0 = \langle \hat{P}^\dagger \rangle = \langle \hat{P} \rangle \quad , \quad (20)$$

where angular brackets denotes the expectation value. We will use the Hill-Wheeler coordinates [23]

$$\beta = \pm \sqrt{q_0^2 + q_2^2} \quad , \quad \gamma = \arctan \left( \sqrt{2} \frac{q_2}{q_0} \right) \quad . \quad (21)$$

We use the standard HFB formalism as can be found in Ref. [2]. Denoting the quasi-particle creation operators by  $b_k^\dagger$ , we find that for a small fluctuation (labelled by the two-quasi-particle index  $kk'$ ) around a given HFB state we have to second order

$$E = \langle \hat{H} \rangle \quad , \quad (22)$$

$$H_{kk'}^{[20]} = \langle b_{k'} b_k \hat{H} \rangle \quad , \quad (23)$$

$$\mathcal{A}_{kk'l'l'} = \langle b_{k'} b_k \hat{H} b_l^\dagger b_{l'}^\dagger \rangle \quad , \quad (24)$$

$$\mathcal{B}_{kk'l'l'} = \langle b_{k'} b_k \hat{H} b_l b_{l'} \rangle \quad . \quad (25)$$



Here  $E$  denotes the HB vacuum energy,  $H^{[20]}$  denotes the gradient of the energy surface at that point and the matrices  $\mathcal{A}$  and  $\mathcal{B}$  are the usual QRPA matrices, which are simple related to the mass and potential matrices of the LHE. The QRPA equations may be cast in the form [2]

$$i(\mathcal{A} + \mathcal{B})P^\mu = Q^\mu \quad . \quad (26)$$

$$-i(\mathcal{A} - \mathcal{B})Q^\mu = \Omega_\mu^2 P^\mu \quad . \quad (27)$$

where  $Q$  and  $P$  are canonical coordinate and momentum variables, respectively. Furthermore from equations (27) we deduce

$$(\mathcal{A} + \mathcal{B})(\mathcal{A} - \mathcal{B})Q^\mu = \Omega_\mu^2 Q^\mu \quad , \quad (28)$$

which is equivalent to the LHE equation (4).

As sketched above, there are exact but spurious solutions to the QRPA which are particularly related zero eigenmodes of eigenvalue equation (28). Operators associated with rotational invariance in normal space  $\hat{J}$  and in gauge space  $\hat{N}$ , generate new states which resemble collective excitations, and thus

$$\begin{aligned} [\hat{H}, \hat{N}] &= 0 \quad , \\ [\hat{H}, \hat{J}_x] &= 0 \quad , \quad [\hat{H}, \hat{J}_y] = -\omega i \hat{J}_z \quad , \quad [\hat{H}, \hat{J}_z] = \omega i \hat{J}_y \quad . \end{aligned} \quad (29)$$

The last two terms are zero for the  $J = 0$  ground state, but at finite  $\omega$ ,  $iJ_y$  and  $J_z$  form a canonical pair, a coordinate and a momentum. In that case the set of spurious coordinates is  $\mathcal{F}^s = \{\mathcal{N}, \mathcal{J}_x, \mathcal{J}_z\}$ .

## A. Results

We have first investigated the quality of the projection scheme for the single  $j$ -shell PPQ model. First consider axially symmetric ( $q_{\pm 2} = 0$ ) ALACM, which corresponds to following the lowest QRPA mode as a function of the collective coordinate  $Q$ . The model space is chosen to be small:  $j = \frac{9}{2}$  and  $N = 4$  fermions and with interaction strengths  $\kappa = 1$  and  $\chi = 0.333$ . We have calculated the mean-field parameters along the collective path. The results are shown in figure 1.

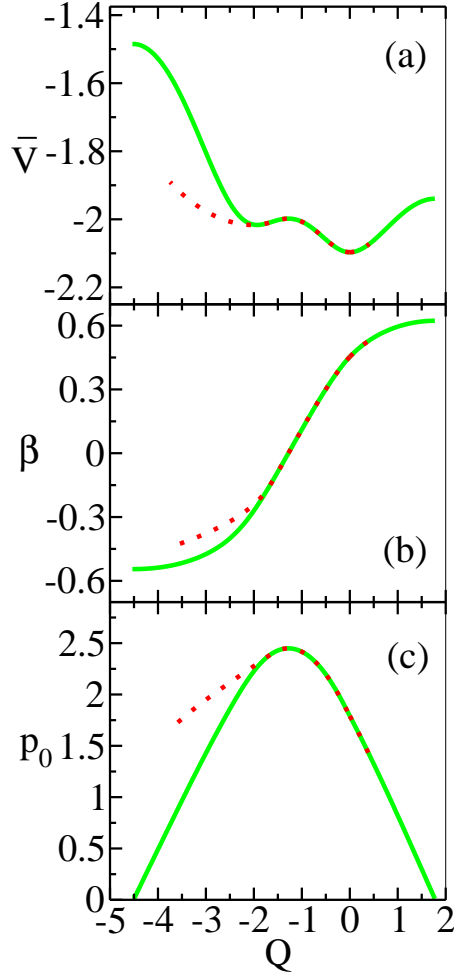


FIG. 1: ALACM following the lowest QRPA mode as a function of the collective coordinate  $Q$ . Figure 1a shows the collective potential  $\bar{V}$ , figure 1b shows the  $\beta$ -deformation and figure 1c shows the pairing parameter  $p_0$ . Each panel shows the naive algorithm (dotted line) and the zero-mode corrected one (solid line). The scale of all displayed quantities is arbitrary, for discussion of these see main text.

For the corrected algorithm (solid line) we identify two minima and three maxima at  $Q \sim \{-2, 0\}$  and  $Q \sim \{-5, -1.25, 2\}$ , respectively. The lowest-energy solution at the starting point  $Q = 0$  corresponds to a prolate minimum and the second minimum at  $Q \sim -2$  is oblate. Comparison of the collective potential with the deformation parameter  $\beta$  and pairing parameter  $p_0$  exhibits the well-known competition between pairing and quadrupole forces. At the boundaries of the collective coordinate  $Q \sim \{-5, 2\}$  the system shows maximal oblate and prolate deformation, respectively, but the pairing field collapses,  $p_0 \sim 0$ . The

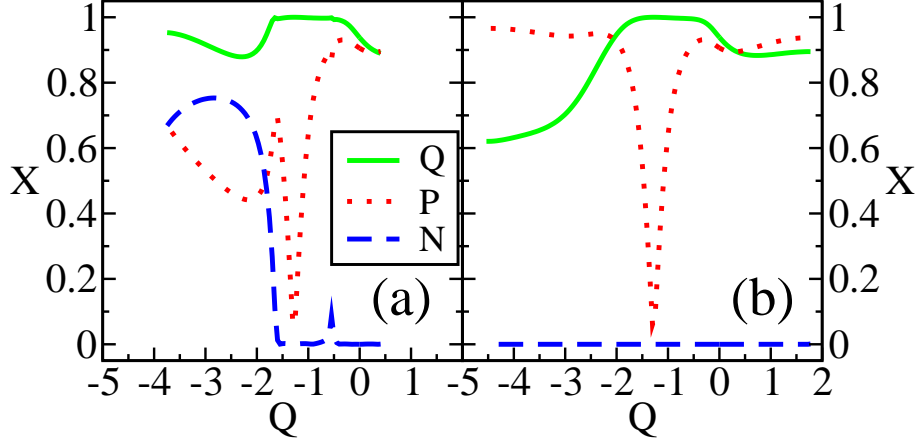


FIG. 2: The overlap of the collective operator with the quadrupole, pairing, and particle-number operators as a function of the collective coordinate  $Q$ . The solid line shows  $X_Q$ , the dotted line  $X_P$ , and the dashed line  $X_N$ , Eq. (30). Figure 2a displays the results for the uncorrected algorithm and figure 2b for the corrected algorithm.

converse is true at the central maximum where the system has collapsed into a state of pure-pairing;  $q_{\pm M} \sim 0$ .

Figure 1 shows clearly that without correctly removing spurious modes (dotted line) the ALACM algorithm fails outside a limited range of the collective coordinate  $-3.75 \lesssim Q \lesssim 0.5$ ; we note that the collective potential and associated mean-field parameters follow a different path from the corrected algorithm (solid line). To better understand this we turn to an analysis of the collective coordinate and calculate the degree of overlap of the collective operator with the operators contained in the Hamiltonian:  $\hat{O} \in \{\hat{Q}_0, (\hat{P}^\dagger + \hat{P}), \hat{N}\}$ ,

$$X_O = \sum_{\alpha} \mathcal{F}_{,\alpha} \mathcal{O}_{\alpha} \quad . \quad (30)$$

The results are shown in figure 2.

For the naive algorithm shown in figure 2a (*c.f.* figure 1c) we see that the collective coordinate is dominated in the region of maximal pairing by a quadrupole-like operator ( $\mathcal{F} \sim Q_0$ ). In particular, where  $Q \sim -1.25$  the pairing-like parameter  $X_P$  tends to zero, and we have a pure  $\beta$ -vibration. From figure 2a we see clearly why the naive algorithm fails at  $Q \sim -1.5$ ; first, we see a sudden increase in the parameter  $X_N$ , and secondly, a sharp change in the pairing-like parameter  $X_P$ . From this it is evident that the spurious coordinate associated with particle number  $\mathcal{N}$  is no longer sufficiently decoupled from the

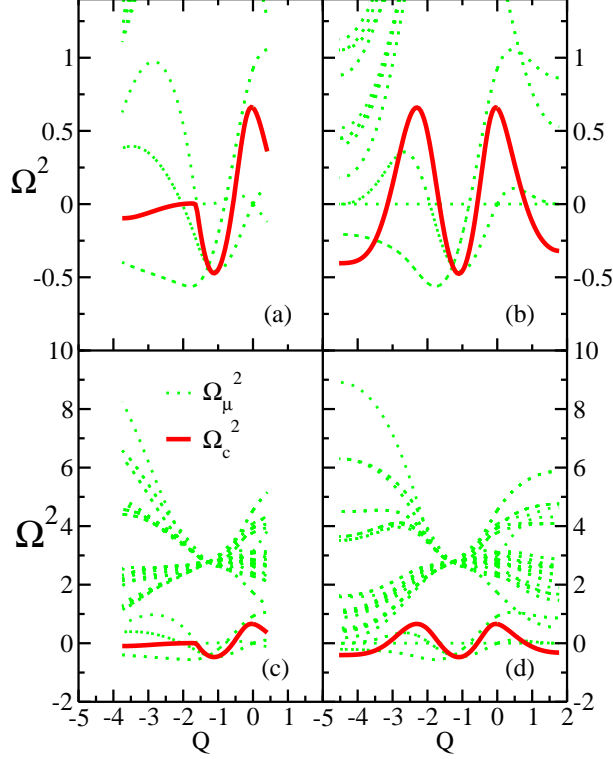


FIG. 3: QRPPA energy eigenvalues squared (dotted lines). The solid line shows the QRPPA mode selected by the path following algorithm. Figures 3a and 3c display results for the uncorrected algorithm and figures 3b and 3d display corresponding results for the corrected algorithm. The scale of all displayed quantities is arbitrary, and determined by the value of  $\kappa = 1$ .

collective coordinate.

This can be seen in figure 3, where we study  $\Omega^2$ , Eq. (28). On the left we show the results of the naive algorithm, and on the right the results from the zero-mode corrected one; the upper two figures differ from the lower two only in scale. It can be seen from figure 3a that at  $Q \sim -1.5$  the energy of the selected eigenmode changes abruptly. At this point we note that the eigenvalue of the collective mode  $\Omega_c^2$  and that of the mode associated with the particle number operator  $\Omega_N^2$  have become degenerate and an avoided crossing of the two levels has occurred. Here the path following algorithm selects the wrong eigenmode, *i.e.* a spurious mode rather than the collective mode, leading the system away from the collective path — this is seen most clearly in figure 4. In figure 3b is shown the corrected result whereby the collective coordinate smoothly crosses the level associated with particle number.

In order to illustrate the source of the problems in the naive algorithm we study both

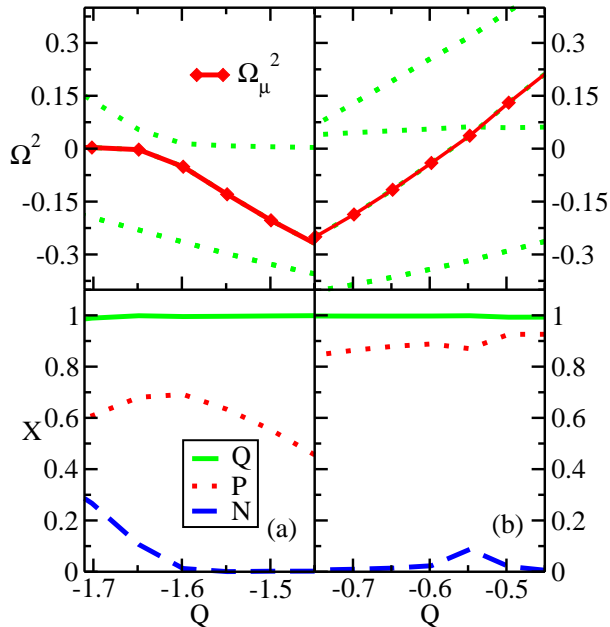


FIG. 4: Analysis of the eigenvalues of the QRPA. Top boxes shows eigenvalues of the QRPA (dotted lines) following the lowest QRPA mode (solid line) as a function of the collective coordinate  $Q$ . Diamond symbols indicate computed points (joined by linear interpolation). Bottom box shows the measure of the overlaps  $X_O$ .

the real and avoided crossings present in figure 3a. We see that the avoided crossing has a large admixture of particle number, and that even the real crossing has a smallish admixture (indicating it is probably a very narrow avoided crossing). We have further investigated the nature of the avoided crossing by using a variety of step lengths. We find that the result is not influenced by changing the step size, and that we can not take steps so large that we run straight through the avoided crossing.

We have investigated changes in the collective potential with respect to variations of the pairing strength  $\chi$  from 0.28 to 0.34. The results are shown in figure 5. From figure 5a we see that the collective potential is higher in energy for lower pairing strength and with a higher maximum relative to the ground-state. Both ends of the collective potential terminate at the same energy, since each of the five systems are identical, that is, where only the quadrupole moment is in effect yielding maximally deformed axially symmetric spheroids. Moreover, we observe from figures 5b-5c that the maximum pairing and  $\beta$ -deformation attained by the system is identical in all cases of pairing strength  $\chi$  as is expected.

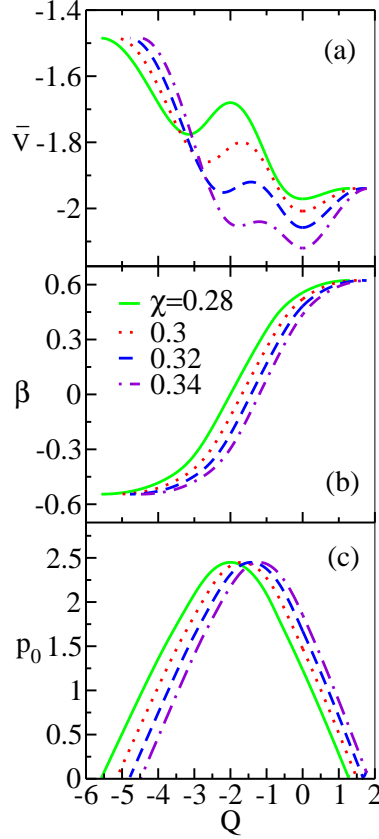


FIG. 5: The result of varying the pairing strength. See figure 1 for an explanation of the subgraphs.

We conclude that the zero-mode-corrected algorithm seems to be able to deal much more efficiently with crossing modes than the naive one. The results obtained with this algorithm have all the properties of the full results, and do not suffer from spurious admixtures and avoided crossings. Since finally we want to understand what happens for rotating nuclei, we must look further at collective motion at non-zero angular momentum.

#### IV. PPQ MODEL AT FINITE ROTATIONAL VELOCITY

To perform a representative test-case of ALACM at finite rotational velocity we have minimised the mean-field energy, and computed the QRPA eigenvalues for values of angular momentum  $0 \leq J_x \leq 6$ , where  $J_x = \langle \hat{J}_x \rangle$ . The results are shown in figure 6.

Figure 6 shows the behaviour of the ground state and its QRPA excitations  $E_\mu = E_0 + \Omega_\mu$ , where  $E_0$  is the ground-state energy and  $\Omega_\mu$  is the  $\mu$ th QRPA frequency. As the angular momentum increases, the pairing field weakens and collapses to zero for  $J_x = 3$ . Until that

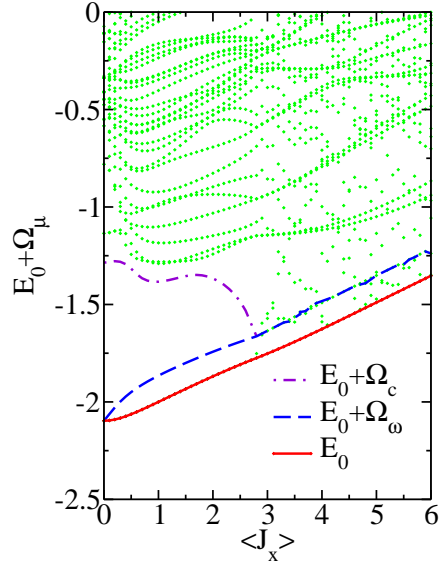


FIG. 6: Partial energy spectra of the PPQ model at finite rotational velocity. Figure shows ground-state energy and a selection of QRPA eigenvalues for fixed quadrupole strength  $\kappa = 10$ , fixed pairing strength,  $\chi = 0.333$ , and rotational velocity  $0 \leq J_x \leq 6$ . The scale of all displayed quantities is arbitrary.

collapse the ground-state (solid line) is degenerate with two eigenmodes associated with the two spurious operators  $\mathcal{N}$  and  $\mathcal{J}_x$ . Thereafter, the only spurious operator is  $J_x$ . The dashed line corresponds to a solution of the QRPA  $\mathcal{F}^\omega$  that appears at the value of the rotational frequency squared ( $\omega_x^2$ ), corresponding to the conjugate pair of operators  $J_y$  and  $J_z$ . Most interesting here, is the appearance of the lowest-lying excitation corresponding to a collective mode  $\mathcal{F}^c$  (dot-dashed line). As the rotational energy increases the collective excitation comes closer to the ground-state.

Until pairing collapse modes mix between pairing and deformation modes. At the point of collapse such modes decouple and we should really solve the ordinary RPA. Nevertheless, even solving QRPA we can easily distinguish between the excitations that change particle number and the deformational modes (continuing lines) which continue to be well behaved into the realm of no pairing. These modes correspond to excitation levels of the standard Nilsson model [2].

### A. Model results at finite rotational velocity

We study angular momentum  $J_x = 2$ , such that the ground-state of the system has non-zero pairing and quadrupole effects (*c.f.* figure 6), we have computed ALACM for the single  $j$ -shell PPQ model at finite rotational velocity following the lowest collective mode of the QRPA. For illustrative purposes we will in the first instance remove only admixtures with the particle number operator.

The quantities  $X_O \in \{X_Q, X_P, X_N, X_{J_x}, X_{J_z}\}$  give the measures of overlap for the collective operator with the quadrupole, pairing, particle number and rotational operators, respectively.

The results are shown in figure 7. As can be seen, the computation has produced values for  $-0.6 < Q < 0.3$  only, due to an instability arising in the path following algorithm discussed further below. For negative values of the collective coordinate we see a decrease in  $\beta$ -deformation (7b) and an increase in  $\gamma$ -deformation (7c), indicating that the system is becoming more triaxial, while the pairing parameter  $p_0$  increases as well (7d). We thus expect the components of the  $M = \pm 2$  quadrupole operator to be important.

As can be seen from figure 7e a spurious admixture connected with  $\mathcal{J}_x$  is causing problems for  $Q < 0$ . As can be seen from figure 7f the eigenvalue of the collective coordinate  $\Omega_c$  (solid line) and the eigenvalue of the coordinate associated with the spurious mode  $\Omega_\omega$  (dashed line) are approximately degenerate. There are therefore two approximately degenerate paths for the path-following algorithm to distinguish, one of which is a spurious solution.

We note one interesting factor outstanding from our discussion of the results thus far. It can be seen that the collective coordinate represented in figure 7f runs approximately parallel with the next higher lying state and though we are unsure of the physical significance of this, it would be interesting to analysis the collective and non-collective coordinates in more detail. To this end, better technology aimed at giving a more detailed description of the system will be introduced below.

We now project out all components associated with spurious modes  $\mathcal{N}$ ,  $\mathcal{J}_x$ , and  $\mathcal{J}_z$ , and secondly, we will compute the measures of overlap associated with all operators of the PPQ model.

We work with the four quantities  $\mathcal{O} \in \{\mathcal{Q}_0, (\mathcal{Q}_{+1} + \mathcal{Q}_{-1}), (\mathcal{Q}_{+2} + \mathcal{Q}_{-2}), (\mathcal{P}^\dagger + \mathcal{P})\}$ . Here on,  $X_0 \in \{X_{J_x}, X_{J_z}, X_N\}$  — the quantities connected with projection — are zero eigenvalues of



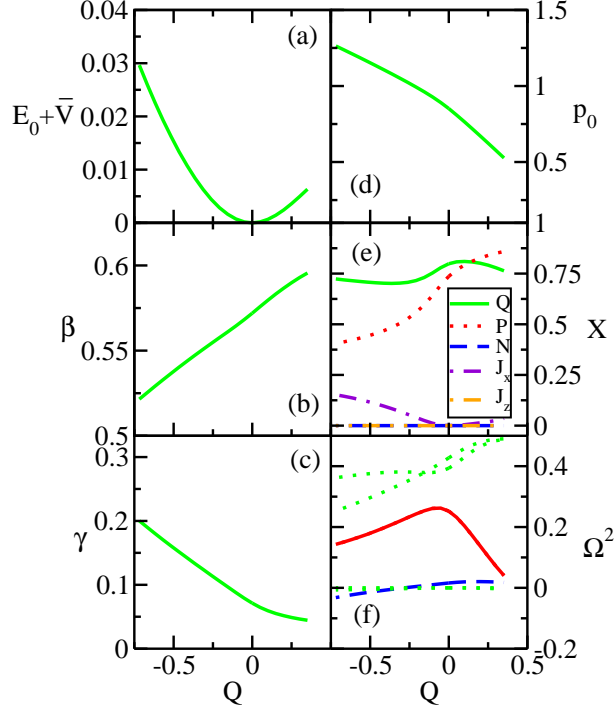


FIG. 7: ALACM for the PPQ model at finite rotational velocity following the lowest QRPA mode as a function of the collective coordinate  $Q$ . The scale of all displayed quantities is arbitrary.

the QRPA eigenvalue equation and otherwise will not be alluded to. The results are shown in figures 8-9.

From figure 8 we see that for positive values of the collective coordinate the collective path has been successfully computed to its end. This is identified by pairing collapse  $p_0 \sim 0$  for  $Q \sim 0.8$  (figure 8d) at a maximum in the collective potential (figure 8a). As the system approaches pairing collapse the  $\beta$ -deformation approaches its maximum value and the  $\gamma$ -deformation approaches a minimal value (figure 8b). In other words, at pairing collapse the system is maximally axially deformed with some small admixture of triaxial deformation. For  $0 \leq Q \lesssim 0.8$  the collective coordinate becomes increasingly more pairing-like for greater values of  $Q$  and less quadrupole-like. In particular, this statement is true of *all* components of the quadrupole operator, *i.e.* for  $X_{Q_0}$ ,  $X_{Q_1}$  and  $X_{Q_2}$ , (solid, dotted and dashed lines respectively) and thus the collective coordinate becomes very pairing-like trying to force the system back toward equilibrium.

For negative values of the collective coordinate the results show an instability at  $Q \sim -1.25$ , where the computation has failed. From figure 8e we see that the collective coordinate

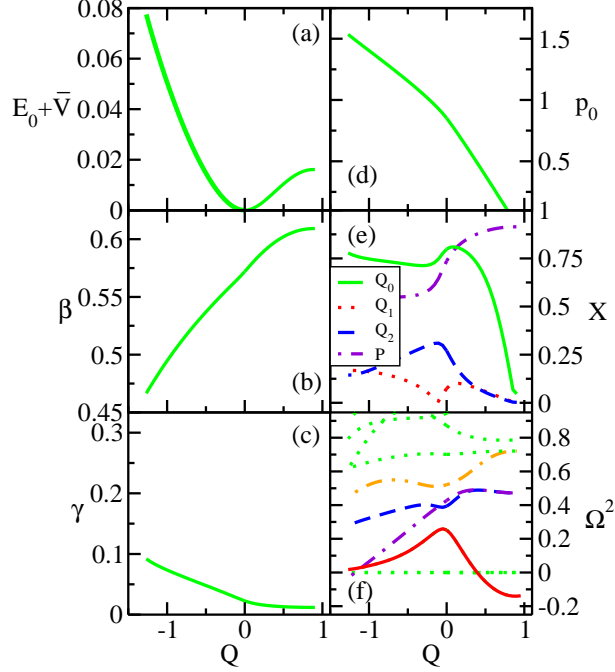


FIG. 8: ALACM for the PPQ model at finite rotational velocity following the lowest QRPA mode as a function of the collective coordinate. The scale of all displayed quantities is arbitrary.

$\Omega_c$  (solid line), becomes degenerate with a second coordinate, labelled  $\Omega_6$  (dashed line). Thus the assumption of a single collective coordinate fails here. This is quite common in this approach, and requires an extended algorithm.

In order to convince ourselves that this is the correct physics, and we are not looking at the spurious admixture problem again, we analyse the QRPA modes  $\Omega_\mu$  in some detail. We have computed the measures of overlap for a few of these modes. At equilibrium there are three spurious modes, and the fourth eigenmode (next highest in energy) is the collective eigenmode we are following  $\Omega_c$ . We concentrate our efforts on the next few QRPA modes, namely, the fifth  $\Omega_5$  (dashed line), sixth  $\Omega_6$  (dot-dashed line), and the seventh  $\Omega_7$  (dot-dot-dashed line, in figure 8d). We note from figure 8f that these modes do not remain in this order for all values of the collective coordinate since there are crossings of energy levels in the energy spectra. The labelling of these modes however, shall remain fixed as defined at  $Q = 0$ , regardless of their subsequent order. The results are shown in figure 9.

We have computed the measure of overlap

$$X_O = \sum_{\alpha} \mathcal{F}_{,\alpha}^{\mu} \mathcal{O}_{,\alpha} \quad , \quad \forall \mu \in \{5, 6, 7\} \quad . \quad (31)$$

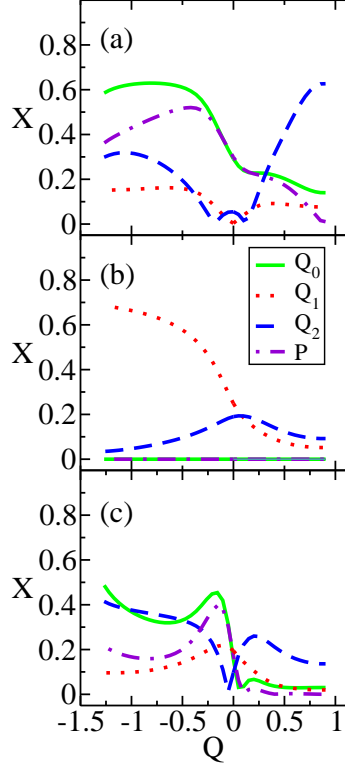


FIG. 9: Analysis of low-lying eigenmodes of the QRPA eigenvalues of the QRPA following the lowest QRPA mode as a function of the collective coordinate. The scale of all displayed quantities is arbitrary. (For discussion of displayed quantities see main text.)

Figure 9 shows the results of our analysis for  $\Omega_5$  (figure 9a),  $\Omega_6$  (figure 9b), and  $\Omega_7$  (figure 9c). In each sub-figure is shown the measures of overlap  $X_{Q_0}$  (solid line),  $X_{Q_1}$  (dotted line),  $X_{Q_2}$  (dashed line), and  $X_P$  (dot-dashed line).

The fifth eigenvalue (figure 9c) and seventh eigenvalue (figure 9a) both exhibit a complex arrangement of all measures of overlap, whose evolutions are not especially discernible; we will return to this later. The sixth eigenmode, figure 9b, contains exclusively admixtures of  $X_{Q_1}$  and  $X_{Q_2}$  meaning that this is a mode that drives both  $\gamma$ -deformation ( $\hat{Q}_{\pm 2}$ ) and tilting ( $\hat{Q}_{\pm 1}$ ). At the point of instability,  $Q \sim -1.25$ , the tilting character is particularly strong.

## V. SUMMARY AND OUTLOOK

In this article we have investigated ALACM using the LHA for the single  $j$ -shell PPQ model. We have computed the collective path, as well as a variety of characteristics of the

mean-field as a function of a single collective coordinate. In order to analyse the collective coordinate in more detail we introduced the measures of overlap, which turned out to be an indispensable tool to analyse the collective coordinate especially in regions where energy levels become degenerate. We introduced a projection technique to remove spurious admixture, which works by projecting a subspace out of the computed mass matrix and potential matrix free from spurious admixture. This method is easily extended to remove the admixture of any finite number of spurious modes. The mixing of spurious modes with the collective mode brings to light an inadequacy of our initial assumption that all modes are approximately decoupled from the collective coordinate.

Using the LHA, collective motion was shown to be non-linear in nature and dominated by neither pairing nor quadrupole degrees of freedom exclusively. Rather, the system self-selects either pairing, or quadrupole, or an admixture of the two to dominate the dynamics and thus select how best the system deforms. More especially, we have found the remarkable feature of a shorter collective path for stronger pairing strength which is not an obvious result.

This leads us to an important limitation, namely, that a single collective coordinate is not sufficient to describe ALACM in regions where the collective coordinate undergoes real crossings with other physical solutions which mix with the collective coordinate. Furthermore, in the course of this investigation we have stumbled across the apparent importance of tilting solutions arising in the quadrupole moment.

We have not computed the covariant derivative of the potential, but we have rather computed a truncation of this which leaves a normal derivative and losing some terms. These terms may well be more important than we suspected at the start. This is something we would like to investigate further. In addition to this, we have attempted to work within the full configuration space available in order to allow a large set of degrees of freedom to contribute to the dynamics. It is worth mentioning here that work on a semi-realistic approach to ALACM using the PPQ model and incorporating many  $j$ -shells [14] uses a truncated QRPA which inadvertently avoids handling spurious modes directly. The projected QRPA was introduced as a computational aid where it was assumed that coupling of normal and spurious modes with the collective coordinate would be small. As we have shown, this assumption may not be correct.

Finally, we note that the LHA is not restricted to a solution for a collective path only,

*i.e.* we could take into account more than one collective coordinate to describe the dynamics of ALACM. The next step is to modify the algorithms we have built, such that they are more apt to describe nuclei at finite rotational velocity using two collective coordinates to determine a collective surface.

### Acknowledgements

This research was funded by the EPSRC and a UMIST scholarship scheme.

- 
- [1] J. P. Blaizot and G. Ripka, *Quantum Theory of Finite Systems* (MIT Press, Berlin, 1986).
  - [2] P. Ring and P. Schuck, *The Nuclear Many-Body Problem* (Springer-Verlag, Berlin, 1980).
  - [3] A. Bohr and B. Mottleson, *Mat. Fys. Medd. Dan. Vid. Selsk* **30**, 1 (1955).
  - [4] M. Baranger and K. Kumar, *Nucl. Phys.* **62**, 113 (1965).
  - [5] M. Baranger and K. Kumar, *Nucl. Phys. A* **110**, 490 (1968).
  - [6] M. Baranger and K. Kumar, *Nucl. Phys. A* **110**, 529 (1968).
  - [7] M. Baranger and K. Kumar, *Nucl. Phys. A* **112**, 241 (1968).
  - [8] M. Baranger and K. Kumar, *Nucl. Phys. A* **112**, 273 (1968).
  - [9] G. D. Dang, A. Klein, and N. R. Walet, *Phys. Rep.* **335**, 93 (2000).
  - [10] T. Nakatsukasa and N. R. Walet, *Czech. J. Phys.* **48**, 813 (1998).
  - [11] T. Nakatsukasa and N. R. Walet, *Phys. Rev. C* **57**, 1192 (1998).
  - [12] T. Nakatsukasa and N. R. Walet, *Phys. Rev. C* **58**, 3397 (1998).
  - [13] M. Kobayasi, T. Nakatsukasa, M. Matsuo, and K. Matsuyanagi, *arXiv:nucl-th* **0001056**, (2000).
  - [14] D. Almehed and N. R. Walet, *Phys. Rev. C* **69**, 024302 (2004).
  - [15] D. Almehed and N. R. Walet, *Phys. Lett. B* **603**, 163 (2004).
  - [16] T. Nakatsukasa, N. R. Walet, and G. D. Dang, *Phys. Rev. C* **208**, 90 (1999).
  - [17] D. Almehed and N. R. Walet, *Acta Physica Polonica B* **34**, 2227 (2002).
  - [18] M. Kobayasi, T. Nakatsukasa, M. Matsuo, K. Matsuyanagi, *Prog.Theor.Phys.* **113**, 129-152 (2005).
  - [19] T. Nakatsukasa, N. R. Walet, and G. D. Dang, *J. Phys. G* **21**, 23 (1999).

- [20] A. Klein, N. R. Walet, and G. D. Dang, *Phys. Rev. B* **322**, 11 (1994).
- [21] M. Kobayasi, T. Nakatsukasa, M. Matsuo, and K. Matsuyanagi, arXiv:nucl-th **030451**, (2003).
- [22] H. Mang, B. Samadi, and P. Ring, *Z. Phys.* **A279**, 325 (1976).
- [23] D. L. Hill and J. A. Wheeler, *Phys. Rev.* **89**, 1102 (1953).